

CFD-BASED RESEARCH OF STRAKE EFFECTS FOR LOW SPEED HIGH LIFT CONFIGURATION

Yuan Zhong, Keliang Zhao

(Shanghai Aircraft Design and Research Institute,
Commercial Aircraft Corporation of China, Shanghai 200232, China)

zhongyuan@email.com; zhaokeliang@email.com

Keywords: High Lift Configuration, CFD, Strake, Vortex, Flow Separation

Abstract

The paper used the high lift configuration of the modern civil wing-mounted aircraft as its research object, and researched the effect of the nacelle and the strake under the low speed state. The CFD was chosen for study. Based on three-dimensional time-dependent compressible Reynolds-averaged Navier-Stokes equations, the three stages of the aircraft configuration in high lift state: wingbody (stage 1), wingbody with nacelle and pylon (stage 2), wingbody with nacelle, pylon and strake (stage 3) were simulated and their lift capability together with flow analysis were given. The paper also analysed the reason why the lift capability changes when the nacelle or the strake is added. From the results to the simulation, the strake can improve the lift capability of the civil wing-mounted aircraft at a high angle of attack (AOA) in low speed state.

1 Foreword

It is quite common in present day modern civil wing-mounted aircrafts use high-bypass ratio engines. Though the high-bypass ratio engines provide lower fuel consumption and reduced noise level, they are larger in diameter. Forced by practical limits on landing gear, length and runway clearance, such wing mounted, high-bypass ratio engines increasingly require much closer coupling of these larger engines to the wing. Even with this close coupling of the nacelle, the nacelle/wing assembly is normally designed so that in cruise configuration the airflow around the nacelle causes relatively little disturbance to the airflow adjacent the wing. For the high lift configuration, the aircraft is generally operating

at a high angle of attack. This results in increased interaction of the engine nacelle and wing flow fields, and particularly with closely coupled nacelles, this can degrade airplane performance. The most serious problems relating to engine-wing interference are the reduction of maximum lift capability and stalling angle in the high lift configuration. In the case of swept wing jet transports, this interference typically will result in premature airflow separation of the portion of the wing inboard. Occasionally, the interference will be severe enough that early airflow separation will also be evident on the wing outboard of the nacelle. However, on swept wings typical of the modern transport the inboard interference is generally much more severe.

A strake is a geometrically small device which generates a strong distinct vortex. Placing this strake in a proper way on the nacelle a significant amount of the lift and stalling angle loss can be recovered.

Two ways, the wind tunnel test and the numerical simulation can be used to investigate the strake. Because of the effects of Reynolds number, there may be a big discrepancy between the results of the wind tunnel test of low Reynolds number and the truth. However, the cost of the wind tunnel test of high Reynolds number is huge, and the test takes too much time. Though the current numerical simulation is not fully developed, it simulates the real flight condition and costs much less, furthermore, it is much more convenient. So, the numerical simulation for the strake is valuable considerably.

The main job of the paper is to analyse the effect of the strake and nacelle to the high lift configuration at a high angle of attack in low

speed state by the numerical simulation, and finds the reason of the effect through flow analysis.

2 The Geometric Model and Grid

2.1 The Geometric Model

The paper used the high lift configuration of a commercial civil aircraft to study. There are three stages of the aircraft configuration. As it shows in the figures, the Stage 1 configuration represents the base high-lift configuration with wingbody, slat and flap only, the engine installation is neglected. In Stage 2, a Through-Flow-Nacelle is installed representing a modern high-bypass ratio engine. In the final Stage 3 configuration a nacelle strake is added.

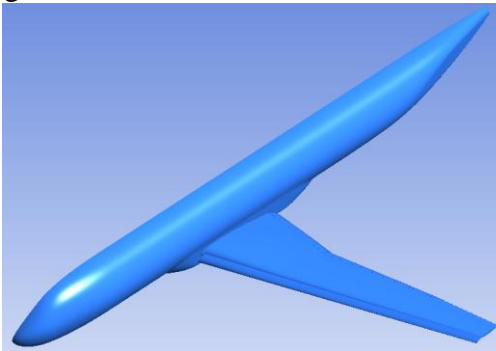


Figure 1. Stage 1

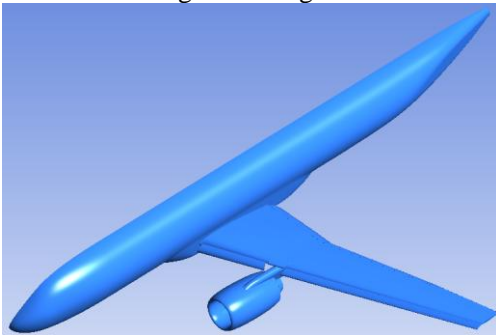


Figure 2. Stage 2

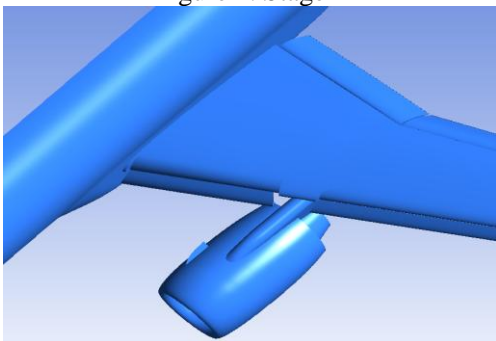
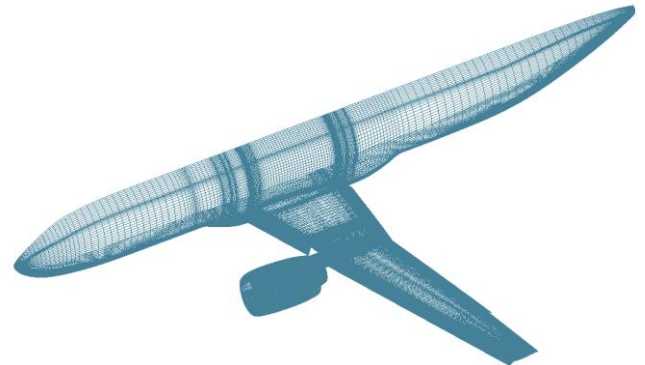


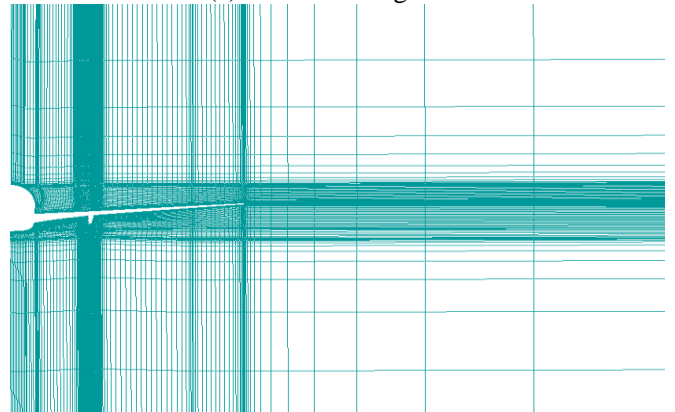
Figure 3. Stage 3

2.2 The Grid

To the complicated geometric shape, it is difficult to generate the body-fitted grid in single domain. Even though the grid is generated constrainedly, the quality may be bad. And the results of the numerical simulation will be affected directly. So, it is quite common in present day to use zone division grid generation technique. Based on the characteristic of the shape, the total flow field is divided to several subdomains. The topology of the grid of each subdomains must be simple. Then generates grid in every subdomains. Zone division grid generation technique makes the structure grid have engineering practicability. Based on the differences of the connection type between block to block, the zone division grid can be divided as three types: 1-1 blocking, patching and overlapping. The paper used the point-to-point patched multi-block technology to generate high quality grid.



(a) The surface grid



(b) The space section grid

Figure 4. Some grids of the paper generated

3 The Calculation Method

The paper solved three-dimensional time-dependent compressible Reynolds-averaged Navier-Stokes equations with third-order upwind-biased flux-difference splitting method and approximate factorization method. The multi-grid technique was employed to accelerate the convergence.

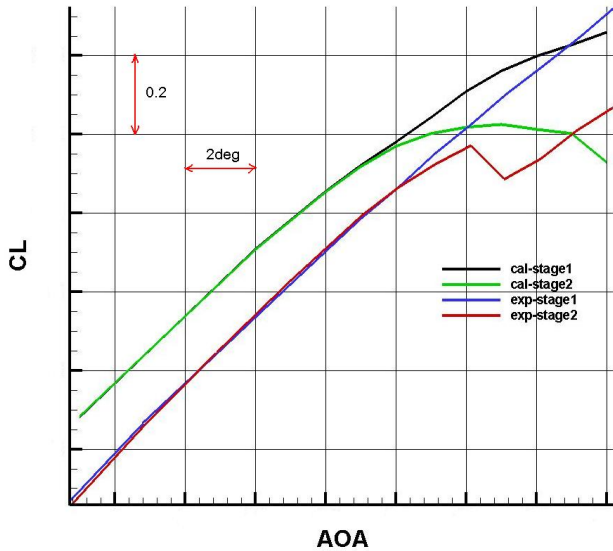


Figure 5. The comparison between calculation and wind tunnel test

Figure 5 shows us the comparison between calculation and wind tunnel test of the stage1 and stage2 configuration when Mach number is 0.2 and Reynold number is $19e6$. We can see that though the absolute value between the calculation and the test has some difference, they match well in the form of the curves and the stall angle. So, the numerical simulation method the paper used is believable.

4 The Calculation Results And Analysis

4.1 The Analysis Between Stage1 And Stage2

As Figure 5 shows, compared to the stage1 configuration, the maximum lift and stall angle of the stage2 are both reduced. That because the nacelle is added.

The figure 6 shows us the cfx-distribution of the stage1 and stage2 configuration when AOA increases. The green color represents the cfx values below Zero. The inboard wing of stage2 appears flow separation, and this leads the

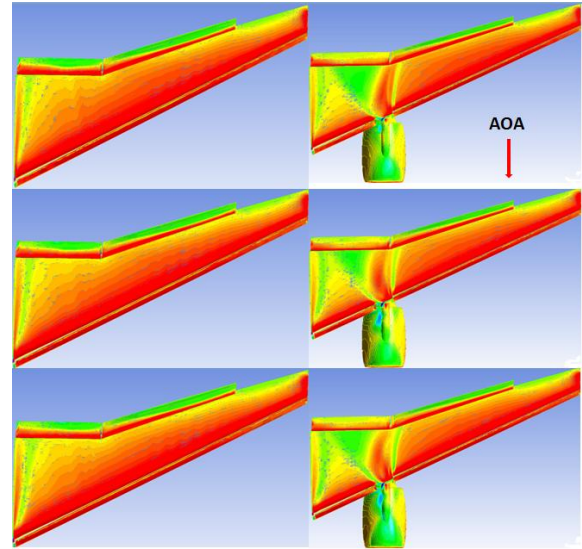


Figure 6. The cfx-distribution of the two configuration lift of the stage2 configuration breakdown.

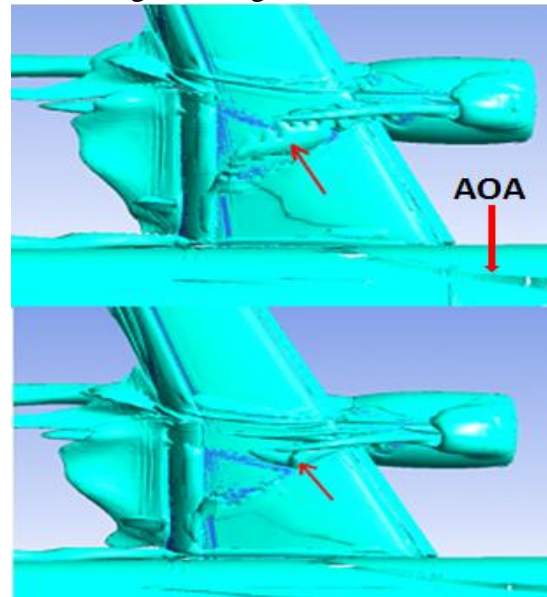


Figure 7. The vortex-distribution of the Stage2 configuration

The figure 7 shows the vortex-distribution of the stage2 configuration when AOA increases. Obviously, the vortex the red arrow point breaks as AOA increases. As the vortex is generated from the pylon district, the paper calls the vortex “the Pylon Vortex”. The region the vortex breaks is the place where the flow separates. So, we can say that the appearance of the flow separation is due to the break of “the Pylon Vortex”. Therefore, we can try to control the break of “the Pylon Vortex” in order to control the flow separation. The strake is the device.

4.2 The Investigation Of The Strake

The stage3 configuration is the shape the strake is added. Figure 8 depicts the calculation results of the three stages. The calculation Mach number is 0.2 and Reynold number is $19e6$.

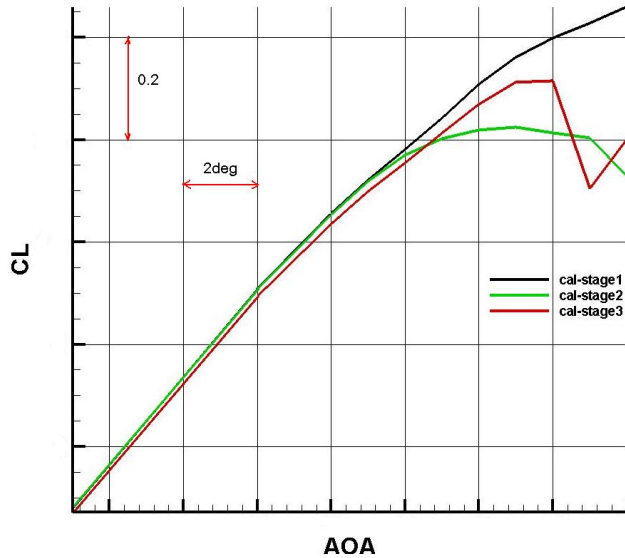


Figure 8. The comparison between three stages

As it shows in the Figure 8, compare to the stage2 configuration, the maximum lift and stall angle of the stage3 are both enhanced obviously. Distinctly, placing the strake in a proper way on the nacelle a significant amount of the lift and stalling angle loss can be recovered.

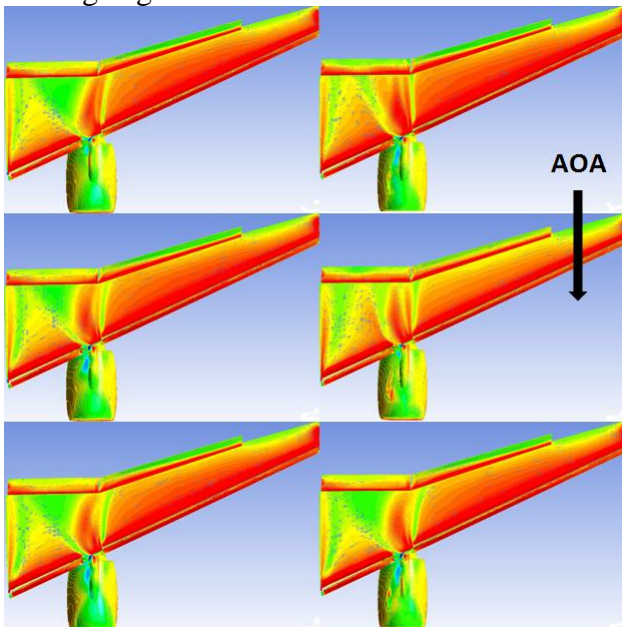


Figure 9. The cfx-distribution of the stage2 and stage3 configuration

Figure 9 depicts the cfx-distribution of the stage2 and stage3 configuration when AOA increases. The left figures are the description of the stage2, and the right figures are of the stage3.

We can see that the flow separation of the stage3 is deferred in connection with the breakdown of the lift is differed. That because the strake is added.

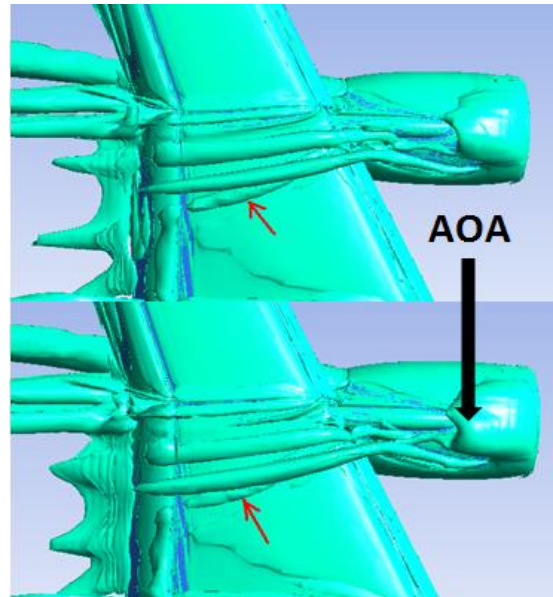
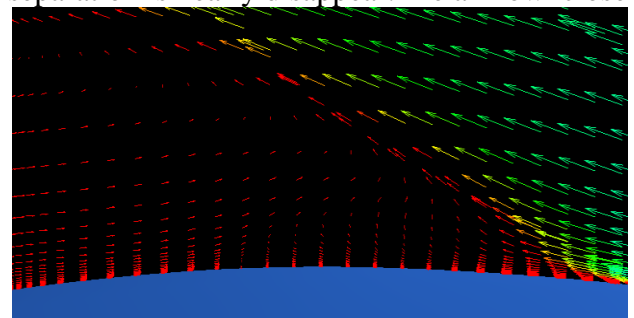


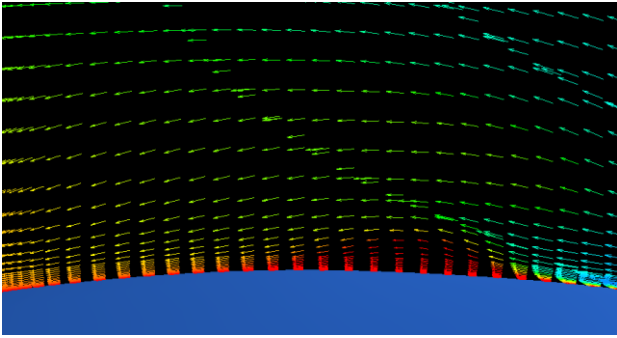
Figure 10. The vortex-distribution of the Stage3 configuration

Figure 10 depicts the vortex-distribution of the stage2 configuration when AOA increases. The angles of Figure 10 are the same as the figure 7. The vortex the red arrow pointed is “the Pylon Vortex”. Apparently, “the Pylon Vortex” is enhanced. The vortex the strake generated enhances “the Pylon Vortex”, makes its break deferred. “The Pylon Vortex” is cling to the wing surface, and inject energy to the boundary layer of the wing continually, makes the high energy airstream enter the boundary layer at all time. So, the flow separation is deferred.

Figure 11 depicts the velocity of the section along the airflow direction near by “the Pylon Vortex”. The red depicts the region with low velocity. The flow separation is obvious in Figure (a). In Figure (b), the velocity of the flow is accelerated, and the region of the flow separation is nearly disappear. The airflow close



(a) the stage2 configuration without strake



(b) the stage3 configuration with strake

Figure 11. The velocity of the section along the airflow direction near by “the Pylon Vortex” to the wing surface is deflected to the wing, this can be propitious to restrain the flow separation.

Consequently, the function of the strake is to enhance “the Pylon Vortex” and make the airflow deflect to the wing, which both can defer the flow separation of the inboard wing.

5 Conclusion

Based on the high lift configuration of the civil wing-mounted aircraft, the influence of the nacelle and the strake were investigated, and got several conclusions:

a) Compared to the stage 1 configuration, the maximum lift and stall angle of the stage 2 configuration are both reduced. The reason is that early airflow separation appears on the inboard wing. The premature break of “the Pylon Vortex” leads to the airflow separation.

b) The strake can recover a significant amount of the maximum lift and stall angle loss by placing it in a proper way on the nacelle.

c) The vortex the strake generated can enhance “the Pylon Vortex”, and defers its break. Accordingly, the airflow separation on the inboard wing is deferred. Furthermore, the vortex the strake generated can make the airflow above the inboard wing deflect to the wing, what can also defer the airflow separation.

References

- [1] Baorui Fang. The Aerodynamics layout Design Of Airplane. The Aviation Industry Publishing Company. 1997.
- [2] A.D. Young and A.B. Haines. Scale Effects on Aircraft and Weapon Aerodynamics[M]. AGARD-AG-323.

- [3] H. Frhr. v. Geyr, N. Schade, J. W. v. d. Burg, P. Eliasson and S. Esquieu. CFD Prediction of Maximum Lift Effects on Realistic High-Lift-Commercial-Aircraft-Configurations within the European project EUROLIFT II [J]. AIAA 2007-4299.
- [4] Baoqin Zhang. Separation flow in low speed state[M]. The Edit Group Of Aviation Teaching Materials Publishing Company. 1988.
- [5] Henderson et al. Nacelle/wing assembly with vortex control device. United States Patent, 4685643[P]. Aug. 11, 1987.
- [6] Mouji Liu et al. The Regula Wing And The Separation Flow Of Vortex[M]. Beijing: The BeiHang Publishing Company, 1988:1-262.
- [7] Fengwei Li, Qin E, Jie Li, Guowei Yang. The Grid Generation Tecnique Of The Complicated Configuration. The Aerodynamics Journal, 16(1), 1998.
- [8] Wilcox, D.C.. Turbulence Modeling for CFD[M]. DCW Industries, Inc., 5354 Palm Drive, La Canada, Calif., 1998.
- [9] Guangning Li. The Numerical Resolution Of Three-Dimensional Navier-Stokes Equations And The Application And Research Of Spalart-Allmaras Turbulence Model. The Papers of Master's Degree Of Northwestern Polytechnical University, 2006.
- [10] Caoqun Liu. The Multi-Grid Method And Its Application In Hydromechanics. The Thinghua University Publishing Company. 1995.

Copyright Statement

The authors confirm that they, and/or their company or organization, hold copyright on all of the original material included in this paper. The authors also confirm that they have obtained permission, from the copyright holder of any third party material included in this paper, to publish it as part of their paper. The authors confirm that they give permission, or have obtained permission from the copyright holder of this paper, for the publication and distribution of this paper as part of the ICAS2012 proceedings or as individual off-prints from the proceedings.